JOURNAL OF PROPULSION AND POWER
Vol. 12, No. 6, November–December 1996

# Fluctuation of Arcjet Plume Properties

Jeffrey A. Pobst*
*Hughes STX Corporation, Edwards Air Force Base, California 93524-7660*
Ronald A. Spores†
*U.S. Air Force Phillips Laboratory, Edwards Air Force Base, California 93524-7160*
and
John H. Schilling‡ and Daniel A. Erwin§
*University of Southern California, Los Angeles, California 90089-1191*

**Physical properties in a 1-kW hydrogen arcjet plume are observed to fluctuate when power is supplied by flight-type high-frequency switching power electronics. The arcjet power processing unit (PPU) is observed to modulate electron density, electron temperature, and atomic excited state emission. Electron density and temperature are measured temporally by employing a triple langmuir probe in the arcjet plume. Emission is observed using spectroscopy techniques. Velocity fluctuations are also detected, though they appear not to be directly linked to the PPU frequency. Determination of species velocity using time-of-flight techniques is described and a connection between the plume emission and the electron temperature is discussed.**

## Nomenclature

FWHM = full width at half maximum
$H\alpha$ = Balmer $\alpha$ hydrogen transition from $n = 3$ to $n = 2$
$n_e$ = electron density
RC = resistor–capacitor
$T_e$ = electron temperature
$V_{d2}$ = differential voltage between probes 1 and 2
$\lambda$ = wavelength
$\nu$ = velocity

## Introduction

ARCJETS are expected to play an increasing role in satellite propulsion needs, primarily stationkeeping and on-orbit maneuvering in the near term. While the technology is considered viable enough to be deployed on a Telstar IV communications satellite for stationkeeping,[1] arcjet technology is far from maturity. After stationkeeping, one of the next steps for electric propulsion will be to satisfy repositioning and orbit transfer missions. With the upcoming Electric Propulsion Space Experiment (ESEX) flight test of a high-power arcjet in late 1997,[2] high-power arcjet technology is being further advanced to fill this niche. However, to compete successfully with chemical propulsion systems for these missions, further improvements in arcjet propulsion systems are still required.[3] If needed improvements in the performance level and efficiency of arcjets are to be achieved, an increased understanding of the fundamental physical processes that govern the operation of an arcjet is essential.

To increase the overall efficiency of an arcjet, it is important to understand the major energy losses, of which frozen flow is believed to be a dominant factor. Frozen flow losses of atomic species include unrecovered dissociation, electronic excited states, and ionization. In addition, molecular species have rotational and vibrational energy states that are not fully converted to kinetic energy. Information pertaining to the frozen flow energy distribution of an arcjet would be beneficial for both designing next-generation thrusters and for comparison purposes with numerical models.

Although much research, both experimental and numerical, has been conducted on arcjet plume characterization over the last 30 years, almost all previous studies assume that the arcjet operates in a steady-state mode. When current is provided by a flight-type, high-frequency, switching power supply, however, the current delivered to the arcjet modulates at the power processing unit (PPU) switching frequency. How this current modulation affects overall arcjet thruster performance is presently unclear. Modulation is thought to potentially play a role in electrode erosion effects,[4] but it must still be resolved how fluctuations affect the more dominant frozen flow issues of dissociation, ionization, and in the case of molecules, vibrational and rotational energy levels.

One of the goals of this work is to provide more insight into the time-dependent arcjet behavior. To address this we present time-resolved measurements of the excited state atomic hydrogen emission in the plume, electron temperature, electron density, and hydrogen velocity. This type of information can indicate gas physics phenomena that are normally averaged when steady-state measurements are taken. For example, measurement of the plume velocity fluctuations provides a velocity correction for the interpretation of steady-state Doppler-broadened temperature measurements. These results also provide critical data for comparisons with numerical work.

Thirty years ago, arcjet emission was used by researchers to estimate fluctuations in species velocity.[5] The uncertainty in this approach was quite large and the technique was not further developed for use in arcjet plumes. To obtain accurate velocity fluctuation data in an arcjet plume, it became necessary to develop a new velocity diagnostic applicable for discerning temporal changes in velocity. This diagnostic, called current modulation velocimetry (CMV), is time-resolved and is based

Portions of this Paper were presented as Paper 92-3238 at the AIAA/SAE/ASME/ASEE 28th Joint Propulsion Conference, Nashville, TN, July 6–8, 1992; as Paper 93-128 at the 23rd International Electric Propulsion Conference, Seattle, WA, Sept. 13–16, 1993; and as Paper 94-2742 at the AIAA/ASME/SAE/ASEE 30th Joint Propulsion Conference, Indianapolis, IN, June 27–29, 1994; received Nov. 2, 1994; revision received Feb. 15, 1996; accepted for publication Aug. 17, 1996. 

*Senior Scientist, U.S. Air Force Phillips Laboratory, Propulsion Directorate. Member AIAA.
†Research Engineer, Propulsion Directorate. Member AIAA.
‡Graduate Research Assistant, Department of Aerospace Engineering. Student Member AIAA.
§Associate Professor, Department of Aerospace Engineering. Member AIAA.

upon manipulation of the current to the arcjet. CMV is inexpensive, fairly easy to operate, and is fully time-resolved, allowing the study of velocity fluctuations in the arcjet plume. Presently, there is no other single shot velocity measurement technique that is applicable to arcjet plumes.

The principal velocity diagnostic presently being used for arcjets is continuous wave laser induced fluorescence (LIF),[6,7] which provides accurate mean velocity measurements, but has very limited temporal resolution. Although the CMV technique employs spatial averaging over a distance of several millimeters, temporal resolution is a few microseconds, enabling plume velocity fluctuations to be measured.

## Experimental Setup

This work employed the 1-kW arcjet designed by NASA Lewis Research Center[8] and is identical to those previously used in many 1-kW arcjet research efforts.[6,7,9] The engine was powered by a 1-kW switching PPU with a 16.67-kHz clock frequency. The propellant used was hydrogen.

Emission measurements took place at two sites under different vacuum conditions. Initial emission measurements were made at the 1.5 × 1 m chamber at the University of Southern California's Department of Aerospace Engineering at an operating pressure of about 135 Pa. Flow rates of 8–10 standard liters per minute (slm) were pumped by a 280 l/s Roots–Stokes combination. Further emission measurements and all triple-probe and current modulation velocimetry were conducted at the U.S. Air Force Phillips Laboratory's Electric Propulsion Lab. Similar flow rates were pumped by a 9300 l/s Roots–Stokes combination, and chamber pressures ranged from 4 to 7 Pa. Fluctuation of emission was observed to be similar in both background pressure conditions.

At both locations, the propellant flow was measured with a thermal-conductivity mass flow meter, calibrated with accuracy ±3% by filling the known plenum volume to a specified pressure and temperature. Engine operating voltage and current were obtained using a parallel 100-kΩ resistive divider and 0.01-Ω series resistor, respectively.

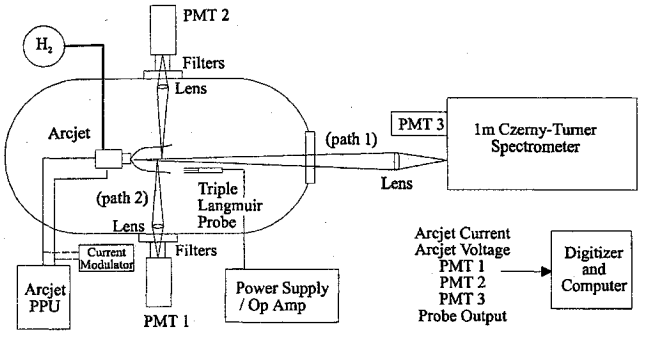


**Fig. 1 Experimental setup.**

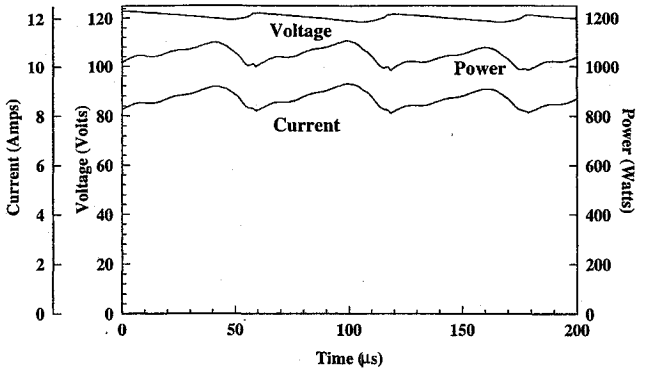


**Fig. 2 Arcjet voltage, current, and power waveforms under typical PPU operating conditions.**

Figure 1 shows the experimental setup used for triple-probe and emission measurements. The arcjet is mounted on a three-axis translation stage, while the optics and probes are fixed. Data from the probes and the photomultiplier tubes (PMTs) are captured on one of two transient digitizers and analyzed on a personal computer.

Initial emission measurements utilized a 1-m Czerny–Turner scanning spectrometer, which collected light from the axial direction (path 1). Light was collected in the radial direction (path 2) using only narrow-band interference filters to select the entire Balmer $\alpha$ ($\lambda$ = 6563 Å, $n$ = 3 to $n$ = 2 transition) or Balmer $\beta$ ($\lambda$ = 4863 Å, $n$ = 4 to $n$ = 2 transition) lines of atomic hydrogen, as well as several orders of neutral density filters and an aperture to select a roughly 1-mm-diam cone of emission. For initial emission measurements only one radial PMT was used, whereas the current modulation velocimetry technique required the use of both radial PMTs. The PMT signals were terminated in 1 kΩ. The trigger for the experiment was the PPU clock signal, i.e., the SYNC signal of the PPU control IC.

A typical plot of arcjet voltage, current, and power is shown in Fig. 2. The current ripple is seen to be about 20%. The voltage ripple is much smaller, about 3%, and 180 deg out of phase with the current ripple. This is consistent with dc operating characteristics of arc devices.[10] The power exhibits approximately 14% ripple, which may be considered an ac component of the propellant heating mechanism.

## Electron Density and Electron Temperature Fluctuations

A triple langmuir probe[11,12] was used to measure the electron temperature and electron density during the PPU switching cycle. The technique used to interpret the triple-probe results and the explanation of triple-probe theory is principally taken from Tilley et al.[11] This diagnostic was chosen because of its simplicity of data reduction and its ability to instantaneously follow fluctuations of the plasma properties in the arcjet plume. A triple-probe consists of three langmuir probes that are electrically set up so that no voltage potential sweeps of the probes are required. The probes are placed as close together as possible without causing probe-to-probe sheath interaction. The larger control volume of the triple-probe technique (~2 × 2 × 3.5 mm) was not a concern for these measurements since an overall regional effect is being investigated.

The triple-probe schematic, which can be seen in Fig. 3, consists of electronics and three wire electrodes that provide $T_e$ and $n_e$ by measuring the voltage potential of probe 2 ($V_{d2=2-1}$) and the current between probes 1–3. The circuit is floating and all electrodes become negatively biased with respect to the plasma potential because of the higher electron mobility. All potentials are actually measured with respect to the local plasma potential of the arcjet plume; however, the plasma potential value is not needed since it drops out in the equations. The thin sheath limit technique of Chen and Seki-

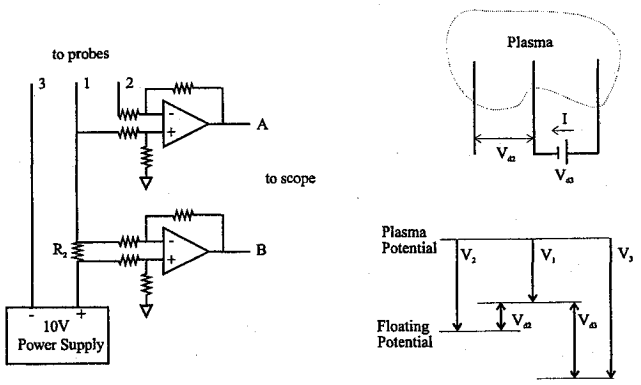


**Fig. 3 Triple-probe schematic.**

guchi[12] is employed in this article; based on error estimates, it was not considered necessary to employ the more accurate exact calculation of Laframboise. A more detailed description on the determination of electron properties relating to the voltage and current is given in a previous publication.[13]

The major sources of triple-probe error, as pointed out in Tilley et al.[11] for the conditions of MPD thrusters, must be re-evaluated for arcjet plasma conditions. The principal assumption employed in the thin-sheath theory is that the ion saturation current is independent of the ratio of the potential of the electrode to the plasma potential. There are several concerns that need to be addressed. One concern is the ion drift velocity perpendicular to the probe axis. However, since probe measurements were only taken on the centerline of the flow axis for these experiments, the component of flow perpendicular to the probe is considered negligible. The ratio of several length scales are considered pertinent: the ratio of probe radius to electron Debye length is calculated as 22.5, the ratio of ion–ion mean free path to probe radius equals approximately 60 and the ratio of probe spacing to electron Debye length is 270. All these ratios are considered acceptable. The probe end-effect parameter was calculated to be on the order of 50, which is also negligible. A further source of probe error is contamination of the electrodes. A glow discharge is typically used for cleaning purposes. For these experiments, the electrodes were placed very close to the arcjet nozzle exit for several seconds. This caused the 0.25-mm tungsten electrodes to glow white hot because of particle–probe collisions, and thus, clean the wire surfaces. The exposed electrode lengths were 0.934 cm and the spacing between probes was 1.5 mm.

Figure 4 shows a comparison of how four arcjet operating parameters behave as a function of time: 1) electron temperature, 2) electron density, 3) arcjet current modulation, and 4) the observed plume emission ripple of the $H\alpha$ line (this will be discussed in the following section). The modulation in the current delivered to the arcjet causes time-dependent variations in several operating parameters. In this case, the PPU current amplitude varies almost 20% ($p$–$p$) around the mean value of 8.2 A and modulates with the PPU switching frequency of 16.6 kHz. The electron temperature is observed to vary over a 20% range about the mean while electron densities fluctuate about 7% throughout the typical modulation cycle. Note that the current modulation, electron temperature, and plume optical signals are all at the same frequency and almost in phase. A time delay between current ripple and both the observed electron temperature and plume emission fluctuations, which were observed at an axial location 2.5 cm downstream of the nozzle exit, is to be expected. There is approximately a 5.2-$\mu$s delay as the gas is convected downstream from the principal arcjet heating zone just in front of the cathode tip. The electron number density, although also strongly correlated with current, is 180 deg out of phase with the electron temperature. However, the observed plume emission is in phase with the electron temperature fluctuations. These observations imply that the electron temperature, rather than the electron density, drives the excited-state populations.

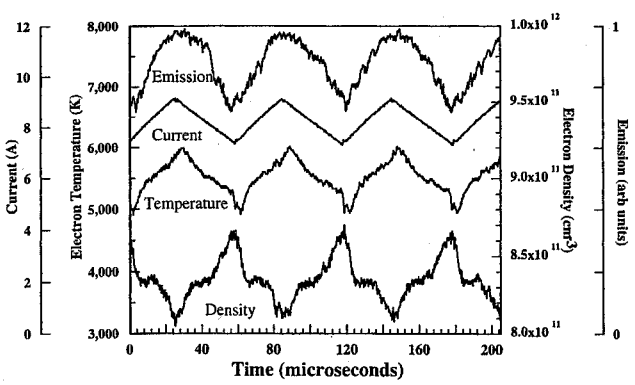


**Fig. 4 Electron temperature, electron density, arcjet current, and plume emission measured in time.**

## Emission Fluctuations

In addition to electron density and temperature, Fig. 4 shows a typical plot of $H\alpha$ emission, measured radially along path 2 (as depicted in Fig. 1) just outside the nozzle exit with respect to the PPU current. The emission ripple is roughly in phase with the current, but larger, about 33% peak-to-peak. The shapes of the two curves are very similar. The presence of an emission fluctuation for a constant mass flow indicates a modulation of excited-state density (hence, of frozen-flow loss) by the PPU switching.

The possibility that the plume velocity is itself modulated because of the time-dependent propellant heating was initially explored by collecting emission in the axial direction (path 1 in Fig. 1). If this effect is significant, it should be visible as a time-varying Doppler shift in emission. Figure 5 shows a contour plot of the spectrally and temporally resolved Balmer $\alpha$ emission. The spectral resolution is provided by the 1-m spectrometer, whose linewidth (FWHM) was measured to be 0.15 Å. The difficulty with this approach is that the measurement collects light from the length of the plume and cannot image a particular radial or axial position; for this reason, light from the arc constrictor region enters the spectrometer as well as light from a large part of the plume.

Horizontal cuts through Fig. 5 give the fluctuating emission at a particular wavelength, whereas vertical cuts give the spectral profile (Doppler and Stark broadened) at an instant in time. Note the large central hump in the spectral profile at all times; the center wavelength of this hump corresponds to the unshifted Balmer $\alpha$ wavelength. This hump may clearly be ascribed to the very low-velocity arc constrictor emission. Below this hump, a horizontal ridge is visible. The center wavelength of this ridge corresponds to a Doppler shift of about 14 km/s, indicating a plume component at that high speed.

While Fig. 5 indicates changes in excited state profiles with respect to the PPU switching frequency, measurements of temperature or direct velocity measurements are not easily inferred as this approach integrates over the emission from the entire plume. What can be observed is that the mean integrated plume velocity does not appear to change significantly with the PPU ripple.

An increase in both emission and electron temperature with respect to arcjet PPU ripple indicates that the excited state population and the electron temperature increase significantly because of small modulations in applied current. Small current variations producing large changes in energy transfer could also lead to shifts in gas velocity. Investigation of propellant

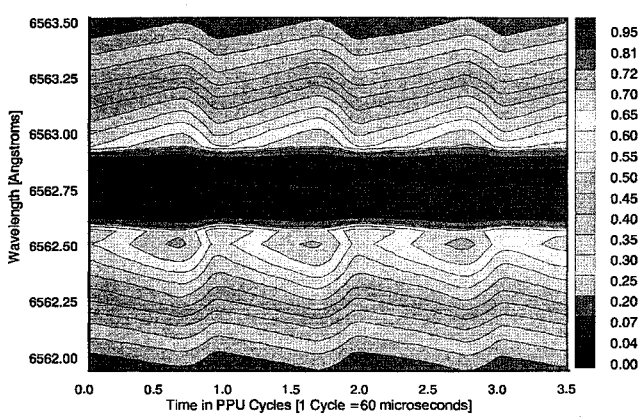


**Fig. 5 Spectral plot in time of Balmer $\alpha$ emission (taken along path 1 in Fig. 1). Colored levels depict fraction of normalized intensity. Note the change in the wings of the large Balmer $\alpha$ peak during the PPU current cycle.**

velocity and the effect on velocity caused by the current ripple was undertaken using two different techniques.

## Velocity from Emission Propagation

Emission measurements were made perpendicular to the axis of propellant flow (path 2 in Fig. 1) and the phase of the emission with respect to the PPU current was observed to vary at different downstream locations in the arcjet plume. Figure 6 shows a group of Balmer $\alpha$ emission plots taken along path 2 at a series of axial stations. The operating conditions were current, 10.0 A; voltage, 119 V; propellant flow, 8.0 slm $H_2$; and chamber pressure, 175 Pa (1.3 torr). The data have been normalized so that all ripples have the same magnitude, and moved vertically to display them in ascending order corresponding to distance from the nozzle exit. The axial separation between each station is 0.5 cm. The data are shown in this manner, discarding the magnitude of both the dc and ac components of the ripple, to emphasize the phase relationship: the phase is retarded from one station to the next.

This retardation indicates that a disturbance or modulation of the excited-state density (for Balmer $\alpha$, the density of the $n = 3$ level of atomic hydrogen) convects at a finite rate. To investigate this, curves 2–11 in Fig. 6 were made to collapse upon curve 1 by a three-parameter transformation, composed of a horizontal translation and a vertical scaling and translation of each curve. Each transformation is optimized to yield minimum integrated least-squares difference between curve 1 and the transformed curve.[14]

Each optimized transformation yielded the retardation (horizontal translation) from curve 1 to the corresponding later curve, as well as its error bar. The error bar is computed from the covariance matrix,[14] assuming that the differences in shape between curve 1 and the other curves are caused by normally distributed noise. These results are shown in Fig. 7. The ordinate is the axial position of each station, whereas the abscissa is the retardation corresponding to the emission measured at that station. The horizontal error bars are the computed retardation errors as just discussed.

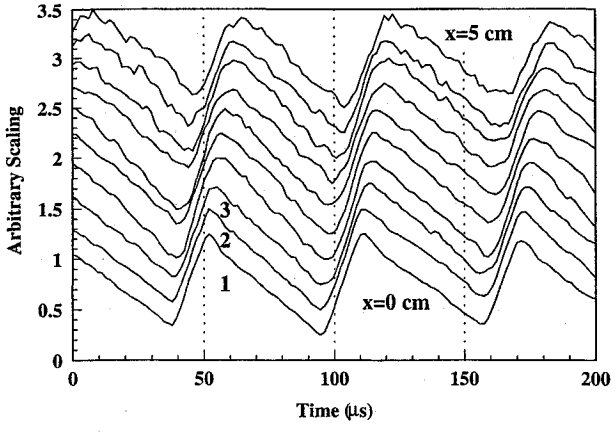


**Fig. 6 Balmer $\alpha$ emission waveforms. Curve 1 was recorded just outside the nozzle exit along path 2, whereas each succeeding curve was recorded 0.5 cm downstream from the previous one.**

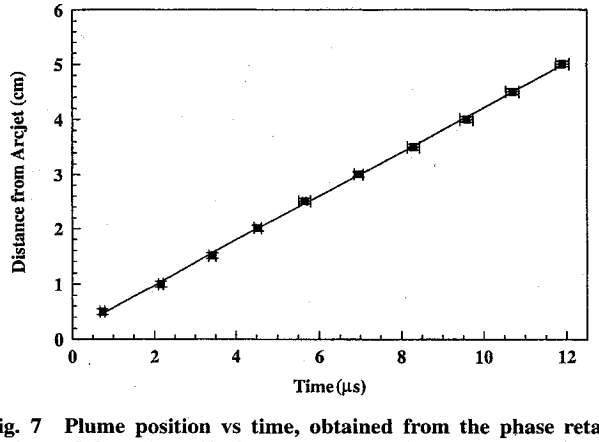


**Fig. 7 Plume position vs time, obtained from the phase retardations of the axially displaced curves of Fig. 6.**

The vertical error bars do not denote random errors, but reflect the finite size of the light collection region; this effect gives rise to a slight convolution or smearing of the raw data.

Figure 7 also gives the least-squares best-fit line corresponding to the data points. As may be seen, the linear fit is excellent. The slope of the line is the plume convection speed, which is seen to be 4.0 km/s under these conditions. This speed seems quite low; note, however, that it is radially averaged and thus includes a large contribution from the boundary layer.

Using the propagation of emission to determine velocity requires measurements of emission ripple phase at many spatial locations. Determination of velocity is then based upon phase differences of the emission at each location with respect to the applied current or the initial emission waveform. To measure velocity more accurately, over a shorter distance, and detect the fluctuation of velocity (if present), a new time-of-flight diagnostic named current modulation velocimetry was developed for use with the arcjet and its PPU.

## Velocity Using Current Modulation Velocimetry

The second velocity technique, CMV, consisted of inserting power circuitry in parallel with the arcjet power feeds to slowly charge up a capacitor and then release the stored energy over a period of microseconds to the arcjet along with the standard PPU applied current. The additional energy in the applied current was then observed as a single event increase in emission that propagated downstream in the plume with the emitting species. This emission event is observed as it passes two optical detectors focused on points within 3 mm of each other. Time of flight of the emission provides an accurate determination of the average velocity during the microseconds it takes to traverse the approximately 3 mm of distance between the two detectors. Relative to other velocity techniques, this measurement provides an essentially instantaneous and accurate velocity measurement with a single event. Multiple measurements can determine variations in velocity at a particular location.

The current spike needed for CMV is generated by a simple RC shunt circuit that is installed in parallel with the arcjet and shown in Fig. 8. Upon closing a switch between this circuit and the arcjet power circuitry, the arcjet voltage appears across the shunt, charging the capacitor over several 1-$\mu$s RC time constants. The shunt current becomes a several-ampere pulse diverting current away from the arcjet, which results in a spiked dropout, and then overshooting back to the arcjet (the total current from the PPU is constant during this time, as it is held constant by an output inductor of several milliHenrys).

An automatic opto-isolated MOSFET circuit allowed computer control of the start time and duration of the modulation to the arcjet current (see Fig. 9). The switch closes based upon a trigger from a pulse generator. The generator issues a pulse when the measured arcjet current reaches a preset level and

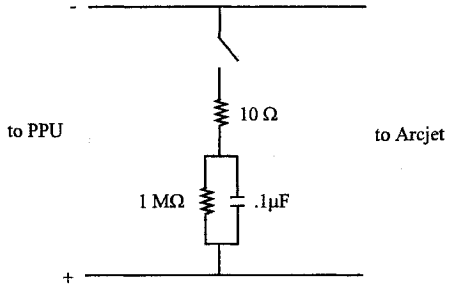


**Fig. 8 CMV circuit.**

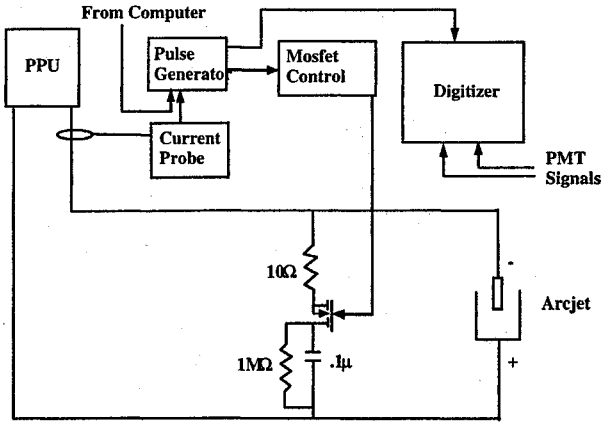


**Fig. 9 CMV automated control with optically isolated MOSFET.**

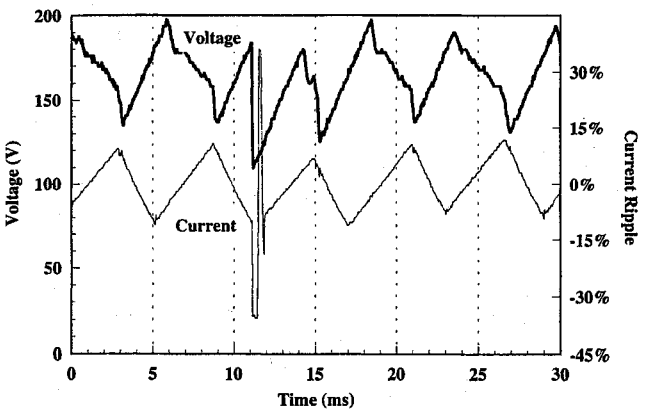


**Fig. 10 Voltage and current during the CMV pulse.**

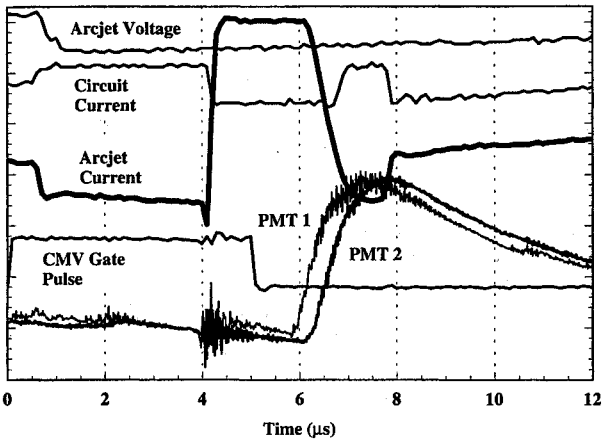


**Fig. 11 Voltage, current, and emission traces during the CMV event.**

after a computer request for an event has been received. This allows the operator to issue a request for a measurement and have that measurement take place the next time the PPU current ripple is at a specified phase.

The positive ring of the current pulse generates a sharp emission spike, which tags a portion of the flow inside the arcjet. The emission spike is delayed with respect to the current pulse by a time interval equal to the integral of $1/\nu$ over the distance from the arc-heating region to the detection station, where $\nu$ is the plume velocity as a function of axial position.

The emission spike is recorded at two different downstream locations using two radial PMT optical trains as shown in Fig. 1. A best-fit transformation between the two digitized emission spikes is determined using the standard Levenberg–Marquardt method.[14] The generated covariance matrix gives a measure of the confidence interval of the best-fit parameters, again assuming the optical signal includes uniform, normally distributed scatter. Error bars indicate the precision of each measured velocity and are computed using a one-standard-deviation confidence interval of the horizontal translation (the time delay between the two emission spikes).

The current and emission spikes are of a few microseconds duration. The time delay between the emission spikes at the two locations can be resolved to within 1 ns, leading to a velocity measurement whose accuracy is in the range 30–60 m/s for plume velocities on the order 5–10 km/s; this accuracy is comparable to those of recent LIF results.[6,7,15]

The velocity measurements obtained with CMV, while still position-averaged over the detector separation (here, 3.29 ± 0.05 mm), are nearly instantaneous. Arcjet velocity has previously been measured by continuous wave[6,7] and pulsed[15] LIF, which provide spatially resolved mean velocity measurements, but have very limited temporal resolution. LIF measurements determine the absorption line shape by scanning in laser wavelength. This takes up to several minutes to resolve the line-shape profile sufficiently to measure precise Doppler shifts, and consequently, accurate velocities.

Figure 10 illustrates the effect of the CMV technique on the arcjet's current and voltage. The PPU-induced arcjet current ripple is briefly interrupted while the capacitor charges. The current then rings upward and significantly overshoots its previous maximum. After quickly dampening, the current begins its previous PPU-induced ripple. Note that the voltage across the arcjet has a characteristic ripple almost 180 deg out of phase with the current. This is expected because of the negative impedance characteristic found in arcjet devices.[16]

Figure 10 also reveals an unexpected behavior of the arcjet voltage that occurs as current is redirected into the capacitor of the RC circuit. The voltage drops suddenly as the current drops and then gradually ramps upward to previous levels without ringing. It then begins its periodic ripple.

In addition to arcjet current and voltage probes, a Hall-effect current probe was placed on the RC circuit. Two digitizing oscilloscopes were used to simultaneously observe several transient signals. These include: the arcjet current and voltage, the current through the circuit when the switch is closed, the gate controlling the switch, and the two emission traces taken from the photomultiplier tubes. The resulting scope traces are shown together in Fig. 11.

The current measured through the RC circuit is complementary to the current going to the arcjet, as expected. When the circuit current drops below its initial level (no current through the circuit), it indicates that current through the circuit has reversed direction and that the capacitor is discharging, which leads to an overshoot of current to the arcjet. The arcjet current rapidly decreases, dropping below its initial level, and a short ring in circuit current is seen. This is followed by a slow rise back up to zero in circuit current and a return to previous ripple behavior in arcjet current.

As noted earlier, the arcjet voltage follows the current as the CMV gate is closed and decreases in value rapidly. As current begins to flow through the circuit, however, the arcjet voltage begins a slow rise back to its previous level, seemingly unaffected by other changes in arcjet current.

Noise in the optical emission, which starts at 4 $\mu$s, is seen simultaneously by both PMTs when the arcjet current first begins to rise. This is then followed by a much more significant increase in Balmer $\alpha$ emission at 6 $\mu$s. This increase occurs at both control volumes, but at different times, seen first at the upstream PMT focal point. The two different emission phenomena seen at 4 and 6 $\mu$s are most likely caused by different excitation processes.

We hypothesize that the optical emission phenomenon that progresses downstream in the plume comes from electron recombination that repopulates the uppermost energy levels of the H atom. The electrons subsequently cascade downward to

repopulate the $n = 3$ excited state, which is then observed by the PMTs as $H\alpha$ emission. This explanation appears valid for the large time-dependent emission peaks that begin at 6 $\mu$s. However, the optical noise seen at 4 $\mu$s must warrant a separate explanation because of its simultaneous observation by both detectors. It is likely that the optical emission at 4 $\mu$s in the arcjet plume is caused by the reabsorption of photons generated at the arc core inside the constrictor region of the arcjet, as suggested by Crofton et al.[17]

Using the current modulation velocimetry technique, arcjet plume velocity measurements were taken along the centerline at a variety of background pressures from 40 mtorr to 1.5 torr. Velocity measurements at each background pressure are very similar between the nozzle exit and about 5 mm downstream, with substantially lower velocities past this point at pressures of 300 mtorr and higher.

Figure 12 presents the lowest and highest pressure cases. Error bars are shown that represent one standard deviation of 10 velocity measurements taken at separate times. We see that the plume velocity is not constant, but fluctuates by several percent or more. Additionally, the trend for axial velocity to decrease with distance from the nozzle is consistent with the expected ambient pressure interactions as seen in the measurements of Liebeskind et al.[6]

In Fig. 12, two points are shown with boxes around them. These boxed points are shown again in Fig. 13, where the 10 individual velocity measurements whose mean and deviation were seen in Fig. 12 are shown separately. The error bars in Fig. 12 are based on the accuracy of measurement of the time delay between a pair of emission traces. Note that this fit error is much smaller than the velocity spread.

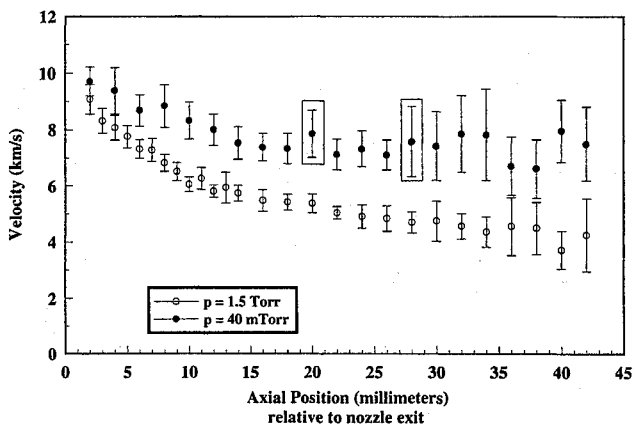


**Fig. 12 Plume velocity vs centerline axial position. Error bars for selected chamber pressures represent the standard deviation spread of velocity measurements taken at a single position.**

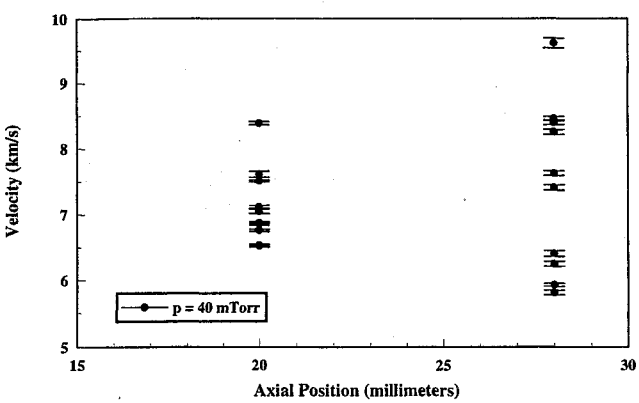


**Fig. 13 Individual velocity measurements (and the individual error in each measurement) that define the standard deviation error bars in Fig. 13.**

In regard to velocity fluctuations, it is worth noting that a time-averaged Doppler line shape will include the effects of fluctuations as well as translational temperature. Therefore, translational temperature obtained assuming a stationary flow is overestimated; however, for the present results, this correction would only amount to a few degrees increase in temperature.

Figure 14 shows the variation of the CMV results for observations at several values of the radial coordinate (distance from the plume axis). It is important to note that these data have not been Abel inverted. Therefore, they represent integrated, radially resolved axial velocities.

To obtain true radial variation of the instantaneous axial velocity, it would be necessary to simultaneously record two traces at each of many radial locations and Abel invert all radial data. Since the experiment only digitized two traces at a single moment, it was impossible to record in this manner. Therefore, it was inappropriate to Abel invert the data obtained here.

The observed fluctuations in velocity might well be linked to the arcjet PPU as seen for the case of emission, electron density, and electron temperature. Verification of this requires that velocity measurements be taken only at one location in the arcjet ripple. Should the velocity fluctuations be linked to the PPU, one would expect little or no fluctuation in the velocity measurement taken at a single phase in the applied current.

To make velocity measurements while linked to the PPU current ripple, a computer-controlled MOSFET gate switch was added to the CMV circuitry as described earlier. This switch allowed precise control of duration and triggering of the current event.

In using this switch a new parameter in CMV operation was required, this being the length of time that the RC circuit was closed (the gate width) in parallel with the arcjet. It was found that gate widths of 3-$\mu$s duration or less caused a change in measured velocity between the two emission collection points in the plume. When the RC circuit is connected to the arcjet for less than 3 $\mu$s, the behavior of current and voltage appears insufficient for the CMV emission to fully take place. The short-gate-width behavior does cause some CMV emission to occur, though at lower intensities than desirable.

These lower velocity measurements are not caused by a lower signal intensity, but are suspect in the fact that the emission shape is less defined and does not appear to have enough time to fully form. It is possible that the recombination processes that repopulate the uppermost electronic levels are incomplete when the circuit is in parallel with the arcjet for short durations. We surmise that the lower velocities result from utilizing a waveform that undergoes change as it traverses between the two imaging control volumes.

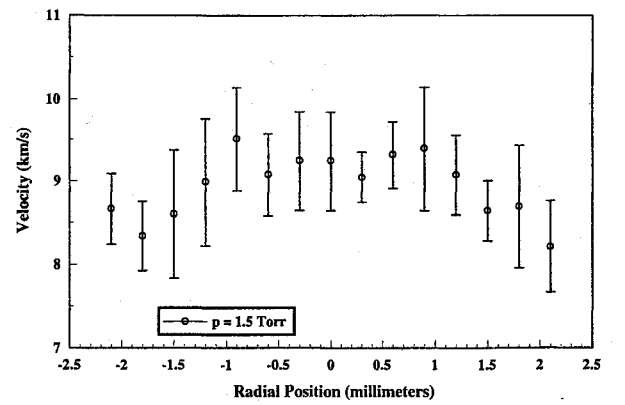


**Fig. 14 Velocity measurements and standard deviation fluctuation ranges taken at radial locations with respect to the centerline of the arcjet nozzle exit.**

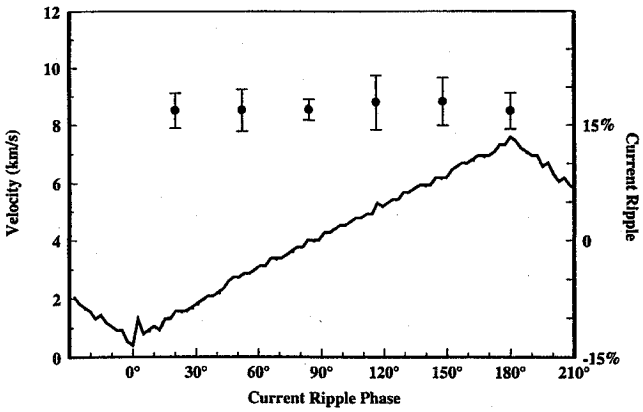


**Fig. 15 Mean velocity and standard deviation of velocity when triggered at a constant point in the PPU current phase at a single position in the arcjet plume.**

It has previously been surmised that the fluctuations shown in Fig. 13 have been a consequence of the oscillating nature of the internal energy dissipation of a 1-kW arcjet resulting from the PPU current modulations. Triggering at a constant PPU ripple level, Fig. 15 shows measured mean velocity and standard deviations taken at several points in the current ripple.

In Fig. 15, no change in mean velocity value or substantive change in fluctuation deviation can be directly related to PPU phase angle. If the velocity is changing with respect to the current ripple, a significant decrease in fluctuation and a variation in mean velocity throughout the PPU modulation cycle should be observed.

There appears to be no connection between the PPU ripple and the mean velocity, and the major cause of the velocity fluctuations in the arcjet plume remains unclear. Attempts at determining a fluctuation frequency through a real-time transformation of the difference between the emission from the two imaging points provide inconclusive results. Determining a fundamental frequency of velocity fluctuation might narrow the possible causes of this phenomenon, though it remains to be seen if a single cause can be pinpointed.

## Conclusions

Fluctuations in arcjet plume properties, observed when using high-frequency flight-type power supplies, are investigated using langmuir probe and emission diagnostic techniques. Fluctuations in electron density, electron temperature, excited state atomic emission, and atomic velocity are detected.

The electron temperature was found to oscillate at the same frequency and almost in phase with the current ripple from the PPU. The electron temperature ranges from a low of 4950 K to a peak value of 6000 K. The electron density was found to fluctuate 180 deg out of phase with the electron temperature, with a peak-to-peak amplitude of 7%.

The electron temperature appears to fluctuate in phase with the arcjet current ripple and the plume optical emission, strongly supporting the hypothesis that plume radiation is predominantly caused by electron recombination, though a small component of emission resulting from photon reabsorption from the arc core is observed.

Propagation of plume optical intensity is shown to enable a simple measure of bulk flow velocity, and an integrated view of the plume spectrally in time shows no significant changes in overall average velocity. An artificial current spike is used to induce a single emission event for a time-of-flight velocity measurement and demonstrates significant local velocity fluctuations. The fluctuations are not observed to be linked to the PPU ripple directly as is the case of emission and electron properties.

## Acknowledgments

This work has been supported by U.S. Air Force Office of Scientific Research (AFOSR) Grant F49620-93-1-01213, AFOSR Task 2308M4, and U.S. Air Force Phillips Laboratory Contract F04611-92-K-0004. The arcjet and power processing unit were provided by NASA Lewis Research Center.

## References

[1]Smith, W. W., "Low Power Hydrazine Arcjet Qualification," 22nd International Electric Propulsion Conf., Viareggio, Italy, Oct. 1991 (Paper 91-148).

[2]Sutton, A. M., "Overview of the Air Force ESEX Flight Experiment," 23rd International Electric Propulsion Conf., Seattle, WA, Sept. 1993 (Paper 93-057).

[3]Vaughan, C. E., and Cassady, R. J., "An Updated Assessment of Electric Propulsion Technology for Near-Earth Space Missions," AIAA Paper 92-3202, July 1992.

[4]Harris, W. J., O'Hair, E. A., Hatfield, L. L., and Kristiansen, M., "Physical Model and Experimental Results of Cathode Erosion Related to Power Supply Ripple," AIAA Paper 92-3837, July 1992.

[5]Van Camp, W. M., Esker, D. W., Checkley, R. J., Duke, W. G., Kroutil, J. C., Merrifield, S. E., and Williamson, R. A., "Study of Arc-Jet Propulsion Devices," NASA CR-54691, March 1966.

[6]Liebeskind, J. G., Hanson, R. K., and Cappelli, M. A., "Laser-Induced Fluorescence Diagnostic for Temperature and Velocity Measurements in a Hydrogen Arcjet Plume," *Applied Optics*, Vol. 32, No. 30, 1993, pp. 6117–6127.

[7]Ruyten, W. M., and Keefer, D., "Two-Beam Multiplexed Laser-Induced Fluorescence Measurements of an Argon Arcjet Plume," *AIAA Journal*, Vol. 31, No. 11, 1993, pp. 2083–2089.

[8]Curran, F. M., and Sarmiento, C. J., "Low Power Arcjet Performance," AIAA Paper 90-2578, July 1990.

[9]Crofton, M. W., Welle, R. P., Janson, S. W., and Cohen, R. B., "Temperature, Velocity and Density Studies in the 1 kW Ammonia Arcjet Plume by LIF," AIAA Paper 92-3241, July 1992.

[10]Pfender, E., *Electric Arcs and Arc Gas Heaters*, edited by M. N. Hirsch and H. J. Oskam, Academic, New York, 1978, p. 291.

[11]Tilley, D. L., Kelly, A. J., and Jahn, R. G., "The Application of the Triple Probe Method to MPD Thruster Plumes," AIAA Paper 90-2667, July 1990.

[12]Chen, S. L., and Sekiguchi, T., "Instantaneous Direct-Display System of Probe Parameters by Means of Triple Probe," *Journal of Applied Physics*, Vol. 36, No. 8, 1965, pp. 2363–2375.

[13]Pobst, J. A., Schilling, J. H., Erwin, D. A., and Spores, R. A., "Time Resolved Measurements of 1 kW Arcjet Plumes Using Current Modulation Velocimetry and Triple Langmuir Probes," 23rd International Electric Propulsion Conf., Seattle, WA, Sept. 1993 (Paper 93-128).

[14]Press, W. H., Flannery, B. P., Teukolsky, S. A., and Vetterling, W. T., *Numerical Recipes: The Art of Scientific Computing*, 1st ed., Cambridge Univ. Press, Cambridge, England, UK, 1986.

[15]Erwin, D. A., Pham-Van-Diep, G. C., and Deininger, W. D., "Laser-induced Fluorescence Measurements of Flow Velocity in High-Power Arcjet Thruster Plumes," *AIAA Journal*, Vol. 29, No. 8, 1991, pp. 1298–1303.

[16]Pencil, E. J., Sankovic, J. M., Sarmiento, C. J., and Hamley, J. A., "Dependence of Hydrogen Arcjet Operation on Electrode Geometry," AIAA Paper 92-3530, July 1992.

[17]Crofton, M. W., Welle, R. P., Janson, S. W., and Cohen, R. B., "Rotational and Vibrational Temperatures in the Plume of a 1 kW Ammonia Arcjet," AIAA Paper 91-1491, June 1991.